

# A laboratory study on the hygroscopic behavior of H<sub>2</sub>C<sub>2</sub>O<sub>4</sub>-containing mixed particles

Qingxin Ma<sup>a,b,c</sup>, Chang Liu<sup>d</sup>, Jinzhu Ma<sup>a,b,c</sup>, Biwu Chu<sup>a,b,c</sup>, Hong He<sup>a,b,c,\*</sup>

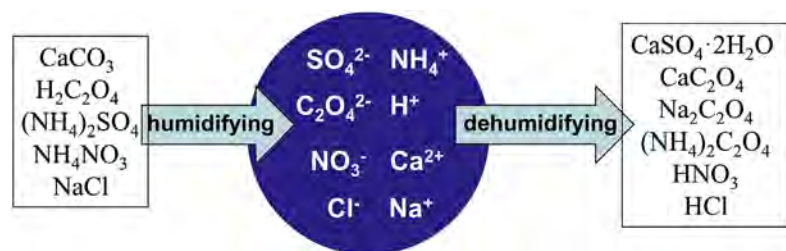
<sup>a</sup> State Key Joint Laboratory of Environment Simulation and Pollution Control, Research Center for Eco-Environmental Sciences, Chinese Academy of Sciences, Beijing, 100085, China

<sup>b</sup> Center for Excellence in Urban Atmospheric Environment, Institute of Urban Environment, Chinese Academy of Sciences, Xiamen, 361021, China

<sup>c</sup> College of Resources and Environment, University of Chinese Academy of Sciences, Beijing, 100049, China

<sup>d</sup> State Key Laboratory of Severe Weather & Key Laboratory of Atmospheric Chemistry of China Meteorological Administration, Chinese Academy of Meteorological Sciences, Beijing, 100081, China

## GRAPHICAL ABSTRACT



## ARTICLE INFO

### Keywords:

Hygroscopic behavior  
Aerosol mixture  
Synergistic effect  
Oxalic acid  
Calcite

## ABSTRACT

The climatic effect of atmospheric particles is greatly dependent on their hygroscopicity and chemical composition. Although the hygroscopic behavior of individual components of aerosol has been widely studied, the effect of coexisting species on the hygroscopic behavior of mixed constituents is still not clear. In this study, we used Raman spectroscopy to investigate how particles with different hygroscopic behaviors affect each other when they are combined together in mixtures. The effect of coexisting hygroscopic components, e.g. NaCl, NH<sub>4</sub>NO<sub>3</sub>, and (NH<sub>4</sub>)<sub>2</sub>SO<sub>4</sub>, on the hygroscopic behavior of externally mixed H<sub>2</sub>C<sub>2</sub>O<sub>4</sub>/CaCO<sub>3</sub> was studied. We found that coexisting NH<sub>4</sub>NO<sub>3</sub> can promote the conversion of H<sub>2</sub>C<sub>2</sub>O<sub>4</sub>/CaCO<sub>3</sub> to CaC<sub>2</sub>O<sub>4</sub>·H<sub>2</sub>O in the humidifying process by providing a deliquesced solution to dissolve H<sup>+</sup> in the oxalic acid matrix. Moreover, competition and blocking effects existed in the case of coexisting (NH<sub>4</sub>)<sub>2</sub>SO<sub>4</sub>. Reactions between (NH<sub>4</sub>)<sub>2</sub>SO<sub>4</sub> and CaCO<sub>3</sub> led to the formation of CaSO<sub>4</sub>·2H<sub>2</sub>O and (NH<sub>4</sub>)<sub>2</sub>C<sub>2</sub>O<sub>4</sub> instead of CaC<sub>2</sub>O<sub>4</sub>. NaCl reacted with H<sub>2</sub>C<sub>2</sub>O<sub>4</sub> in solution to form Na<sub>2</sub>C<sub>2</sub>O<sub>4</sub>. These results suggested that synergistic effects between coexisting components in mixed particles during the humidifying-dehumidifying process may change their chemical composition, mixing state, and hygroscopicity. In addition, chemical reactions should be considered in future studies on the hygroscopic behavior of mixed particles.

\* Corresponding author. State Key Joint Laboratory of Environment Simulation and Pollution Control, Research Center for Eco-Environmental Sciences, Chinese Academy of Sciences, Beijing, 100085, China.

E-mail address: [honghe@rcees.ac.cn](mailto:honghe@rcees.ac.cn) (H. He).

<https://doi.org/10.1016/j.atmosenv.2018.11.056>

Received 11 September 2018; Received in revised form 24 November 2018; Accepted 29 November 2018

Available online 09 December 2018

1352-2310/© 2018 Elsevier Ltd. All rights reserved.

## 1. Introduction

Atmospheric aerosols affect climate directly through scattering and absorption of solar radiation, and indirectly through changing the optical properties and lifetime of clouds by acting as cloud condensation nuclei (CCNs) (Ramanathan et al., 2001) and ice nucleating particles (Tang et al., 2018). Although the sum of the direct and indirect cooling effects of aerosols has been established to be almost equivalent to the warming effect of carbon dioxide, the negative forcing of atmospheric aerosols remains the largest source of uncertainty in predictions of the future global climate (Solomon, 2007). Therefore, a number of studies have focused on the physicochemical properties of aerosols, especially the hygroscopic behavior. In general, solid salt particles that are hygroscopic in nature take up water in the atmosphere and form aqueous droplets. This hygroscopic growth influences the light scattering, cloud formation and precipitation, atmospheric lifetime and chemical reactivity of atmospheric particles (Charlson et al., 1992). The hygroscopic properties of an aerosol also determine which fraction of aerosol particles can act as CCN and thus contribute to the indirect aerosol effect (Pilinits et al., 1995). Due to their great importance, the hygroscopic behavior of aerosol particles as well as the atmospheric processes related to the hygroscopic behavior of aerosol have received much attention.

Atmospheric aerosol is usually found to be a mixture of various inorganic and organic components in field measurements (Andreae et al., 1986; Li and Shao, 2009a, b; Poschl, 2005; Sullivan et al., 2007; Sullivan and Prather, 2007). The hygroscopic behaviors of individual inorganic salts or organic components commonly found in atmospheric aerosols are well characterized nowadays. However, the effect of mixing state on the hygroscopic behavior of coexisting components in mixed aerosol particles remains unrevealed (Hallquist et al., 2009; Wu et al., 2011). The Zdanovskii-Stokes-Robinson (ZSR) model has been applied to predict the hygroscopicity of mixed particles using the volume or mass fraction of each component. For example, the water activity of mixtures of NaCl with  $\text{MgSO}_4$ ,  $\text{Na}_2\text{SO}_4$  or  $\text{MgCl}_2$  was studied (Chan et al., 2000). Good agreement was found between the predictions of the ZSR model and the experimental data over the entire range of water activity for all mixtures studied before crystallization occurred. The hygroscopic growth factors (GFs) of internally mixed NaCl-glutaric acid and NaCl-pinonic acid mixtures measured with a hygroscopicity tandem differential mobility analyzer (H-TDMA) system showed that the GFs of mixtures agreed with the predictions of the ZSR approach (Cruz and Pandis, 2000). Pope et al. also found that the properties of aqueous mixtures of malonic acid and glutaric acid with NaCl could be estimated well based on those of the pure solutions (Pope et al., 2010). However, a recent study found that the ZSR model is not suitable for predicting the hygroscopic behavior of externally mixed components, especially when chemical reactions occur (Ma et al., 2013c). Therefore, the hygroscopic behavior of mixed particles needs further study.

Previous laboratory studies on the hygroscopic behavior of inorganic-organic mixtures mainly focused on the water-soluble constituents. For instance, the effects of dicarboxylic acids (DCAs) on hygroscopic inorganic compounds like  $(\text{NH}_4)_2\text{SO}_4$ , NaCl,  $\text{NaNO}_3$ ,  $\text{MgCl}_2$ ,  $\text{CaCl}_2$ ,  $\text{CaCO}_3$ , etc. in mixtures have been widely studied (Braban and Abbatt, 2004; Brooks et al., 2002; Choi and Chan, 2002; Cruz and Pandis, 2000; Drozd et al., 2014; Laskina et al., 2015; Ma and He, 2012; Ma et al., 2013c; Prenni et al., 2003; Shao et al., 2018; Wang et al., 2017; Wise et al., 2003). Oxalic acid ( $\text{H}_2\text{C}_2\text{O}_4$ ) is the most abundant contributor to DCAs, which represent a significant portion of the organic fraction of aerosols in the atmosphere (Chebbi and Carlier, 1996; Sullivan and Prather, 2007; Wang et al., 2012). It was found that the presence of oxalic acid has no measurable effect on the deliquescence relative humidity of ammonium sulfate due to its lower solubility (Brooks et al., 2002; Wise et al., 2003), but that it apparently inhibits the nucleation of ammonium sulfate (Prenni et al., 2003). However, a recent study by Wang et al. showed that ammonium hydrogen oxalate

( $\text{NH}_4\text{HC}_2\text{O}_4$ ) and ammonium hydrogen sulfate ( $\text{NH}_4\text{HSO}_4$ ) are formed from interactions between  $\text{H}_2\text{C}_2\text{O}_4$  and  $(\text{NH}_4)_2\text{SO}_4$  in aerosols during the dehydration process (Wang et al., 2017). The reaction between oxalic acid and NaCl or  $\text{NaNO}_3$  also occurs in the dehydration process of oxalic acid-containing mixtures, which leads to the formation of  $\text{Na}_2\text{C}_2\text{O}_4$  and volatile inorganic acids like  $\text{HNO}_3$  and HCl (Laskin et al., 2012; Ma et al., 2013c; Wang and Laskin, 2014).

On the other hand, the interaction between soluble components and insoluble mineral dust is still not clear. Field measurement results analyzing Asian dust by single particle mass spectrometry (ATOFMS) showed that oxalic acid was predominantly mixed with mineral dust during transport in the atmosphere (Sullivan and Prather, 2007; Yang et al., 2009). It has been proposed that the origin of DCA/mineral dust mixtures is heterogeneous and aqueous oxidation of DCAs' precursors on alkaline Asian dust surfaces (Sullivan and Prather, 2007). Wang et al. suggested that oxalic acid in coarse mode originated from evaporation from fine mode particles and subsequent condensation/adsorption onto pre-existing coarse particles (Wang et al., 2012). By using X-ray absorption fine structure spectroscopy (XAFS), Furukawa and Takahashi (Furukawa and Takahashi, 2011) found that most of the oxalic acid in mineral mixtures is present in the form of metal oxalate complexes in aerosols, especially Ca and Zn oxalate complexes. Although the affinity between oxalic acid and calcite has been widely proposed, the formation mechanism of metal-complexed oxalate species in mixed mineral dust particles is still not well recognized (Furukawa and Takahashi, 2011). Calcite ( $\text{CaCO}_3$ ) is considered to be a reactive component of mineral dust aerosols. Due to its alkalinity, calcite has a significant neutralization effect on atmospheric acidic constituents, such as  $\text{H}_2\text{SO}_4$ ,  $\text{SO}_2$ ,  $\text{HNO}_3$ ,  $\text{NO}_2$ , and carboxylic acids (Al-Abadleh et al., 2003; Al-Hosney and Grassian, 2005; Crowley et al., 2010; Dentener et al., 1996; Laskin et al., 2005; Ma et al., 2012; Tang et al., 2016; Usher et al., 2003). The interaction between oxalic acid and calcite in mixtures during the humidifying process has also been considered in recent laboratory studies. Gierlus et al. (2012) determined that cloud processes under supersaturation conditions can trigger reaction between mixtures of  $\text{H}_2\text{C}_2\text{O}_4$  and  $\text{CaCO}_3$ , resulting in the formation of  $\text{CaC}_2\text{O}_4$ . Meanwhile, in a previous study (Ma and He, 2012), we found that there exists a synergistic effect in the humidifying process of atmospherically relevant calcium nitrate, calcite, and oxalic acid mixtures. Substitution of strong acid ( $\text{HNO}_3$ ) by weaker acid ( $\text{H}_2\text{C}_2\text{O}_4$ ) occurred when water vapor was absorbed in  $\text{Ca}(\text{NO}_3)_2/\text{H}_2\text{C}_2\text{O}_4$  mixtures. Moreover, coexisting hygroscopic nitrate shows a promotive effect on the reaction between  $\text{H}_2\text{C}_2\text{O}_4$  and  $\text{CaCO}_3$  under ambient conditions by providing an aqueous solution after deliquescence. Since mineral dust represents one of the biggest contributors to atmospheric aerosol, it is necessary to further study the hygroscopic behavior of inorganic-organic mixtures containing mineral dust.

In previous studies, Gierlus et al. (2012) and Laskina et al. (2013) found that Ca oxalate was formed in the internally mixed particles generated by atomizing a suspension of insoluble powder in an aqueous solution. However, the aqueous reaction process was not observed directly. In this study, we prepared externally mixed particles to investigate the aqueous reaction process in the humidifying-dehumidifying process using Raman spectroscopy. Typical atmospheric hygroscopic component, e.g., NaCl,  $\text{NH}_4\text{NO}_3$ , or  $(\text{NH}_4)_2\text{SO}_4$ , were chosen to study whether they were involved in this reaction. The results suggested that, besides cloud process, the chemical reaction between  $\text{H}_2\text{C}_2\text{O}_4$  and  $\text{CaCO}_3$  under unsaturated humidity condition could be also an important pathway for the formation of coated or internally mixed oxalate with mineral dust when hygroscopic components coexist.

## 2. Experimental section

*In situ Raman spectroscopy:* Raman spectroscopy has been widely used to study the hygroscopic behavior of aerosols (Liu et al., 2008; Tang and Fung, 1997). A UV/Vis resonance Raman spectrometer (UVR

DLPC-DL-03) was used to record the in situ Raman spectra, which has been described elsewhere (Liu et al., 2010). The exciting laser was a continuous diode-pumped solid state (DPSS) laser (532 nm) with source power of 40 mW. The spectra resolution was  $2.0 \text{ cm}^{-1}$ . In a typical experiment, particles were placed in an in situ cell and the temperature was 293 K. The relative humidity in the stream was measured by a moisture meter (CENTER 314, China,  $\pm 2\%$  RH,  $\pm 0.1$  K). Each RH point was equilibrated for more than 40 min if not otherwise stated. A humidifying-dehumidifying (H-D) cycle consisted of increasing the RH around the samples from 0 to 95% and then decreasing it to zero.

**Chemicals:** The externally mixed samples were prepared by grinding different components together. The molar ratio of oxalic acid and calcite was unity according to the stoichiometry.  $\text{CaCO}_3$  (AR, Beijing Yili Fine Chemical Co. Ltd.),  $\text{H}_2\text{C}_2\text{O}_4 \cdot 2\text{H}_2\text{O}$  (AR, Beijing Yili Fine Chemical Co. Ltd.),  $\text{NaCl}$  (AR, > 99.5%, Sinopharm Chemical Reagent Co. Ltd.),  $\text{NH}_4\text{NO}_3$  (AR, > 99.5%, Sinopharm Chemical Reagent Co. Ltd.), and  $(\text{NH}_4)_2\text{SO}_4$  (AR, > 99% Beijing Chemical Reagent) were used as purchased. Distilled  $\text{H}_2\text{O}$  was degassed by heating prior to use.

### 3. Results and discussions

#### 3.1. Hygroscopic behavior of mixed $\text{CaCO}_3/\text{H}_2\text{C}_2\text{O}_4$ particles

Fig. 1 shows the Raman spectra of mixed  $\text{H}_2\text{C}_2\text{O}_4/\text{CaCO}_3$  particles before (line a) and after (line b) a humidifying-dehumidifying process. Several peaks at 120, 182, 286, 485, 545, 715, 850, 1088, 1320, 1488, and  $1707 \text{ cm}^{-1}$  are seen. Compared to the spectrum of anhydrous  $\text{H}_2\text{C}_2\text{O}_4$  particles (line c), peaks at 286, 715, and  $1088 \text{ cm}^{-1}$  are assigned to calcite while others are attributed to anhydrous oxalic acid particles (Ma and He, 2012). The assignments of characteristic peaks in various spectra were summarized in Table 1. The spectrum of mixed particles before the humidifying process (line a) is very similar to the spectrum of mixed particles after the humidifying process (line b) without any shifting of peaks or the presence of new peaks. The spectrum of  $\text{CaC}_2\text{O}_4 \cdot \text{H}_2\text{O}$  in the form of whewellite is also shown in Fig. 1 (line d) for comparison (Frost and Weier, 2003). Peaks belonging to  $\text{CaC}_2\text{O}_4 \cdot \text{H}_2\text{O}$  did not appear in the spectrum of  $\text{H}_2\text{C}_2\text{O}_4/\text{CaCO}_3$  (line b), indicating that no reaction took place between oxalic acid and calcite in the humidifying-dehumidifying cycle. Since calcite and oxalic acid are not deliquescent in the range of 0–95% RH, reaction between the two different kinds of solid particles hardly takes place, especially in external mixtures.

It is important to note that the reaction between  $\text{H}_2\text{C}_2\text{O}_4$  and  $\text{CaCO}_3$  has been observed by Gierlus et al. (2012) and Laskina et al. (2013)

**Table 1**

The assignments of characteristic peaks in the spectra of particles.

Raman shift ( $\text{cm}^{-1}$ )	assignment	reference
286, 715, 1088	$\text{CaCO}_3$	Ma and He (2012)
485, 850, 1320, 1488	$\text{H}_2\text{C}_2\text{O}_4$	Ma et al. (2013a)
1464, 1491	$\text{CaC}_2\text{O}_4 \cdot \text{H}_2\text{O}$ (whewellite)	Frost and Weier (2003)
1046	$\text{NH}_4\text{NO}_3$	Ma et al. (2013b)
974, 981	$(\text{NH}_4)_2\text{SO}_4$	Ma et al. (2013b)
1007, 1137	$\text{CaSO}_4 \cdot 2\text{H}_2\text{O}$	Ma et al. (2013b)
1416, 1451	$\text{Na}_2\text{C}_2\text{O}_4 \cdot 2\text{H}_2\text{O}$	Ma et al. (2013c)
1490	$\text{CaC}_2\text{O}_4 \cdot \text{H}_2\text{O}$ (weddelite)	Frost and Weier (2003)

previously. Such a discrepancy is likely to be associated with the differences in experimental conditions and aerosol preparation, as explained by Laskina et al. (2013). In the work of Gierlus et al. (2012) and Laskina et al. (2013), internally mixed particles were generated by a constant output atomizer from an aqueous suspension of calcite and oxalic acid solution, in which  $\text{H}^+$  is available for decomposition of calcite. In contrast, in externally mixed calcite and oxalic acid particles, the  $\text{H}^+$  is fixed in the oxalic acid matrix and does not decompose calcite.

#### 3.2. The effect of $\text{NH}_4\text{NO}_3$ on the hygroscopic behavior of mixed $\text{CaCO}_3/\text{H}_2\text{C}_2\text{O}_4$ particles

The presence of 20 wt%  $\text{NH}_4\text{NO}_3$  can promote the reaction between oxalic acid and calcite during the humidifying process, as seen in Fig. 2. For dry mixed particles, peaks at 1485 and  $850 \text{ cm}^{-1}$  were attributed to  $\text{H}_2\text{C}_2\text{O}_4$ , while peaks at 1088 and  $286 \text{ cm}^{-1}$  were attributed to  $\text{CaCO}_3$  (Ma and He, 2012). The peak at  $1046 \text{ cm}^{-1}$  was assigned to  $\text{NH}_4\text{NO}_3$ . When RH increased to 30%, the peaks at 1485 and  $850 \text{ cm}^{-1}$  shifted to 1496 and  $860 \text{ cm}^{-1}$ , respectively. These shifts were due to the conversion of anhydrous oxalic acid to the dihydrate (Ma and He, 2012). As RH further increased to 50%, the peak at  $1046 \text{ cm}^{-1}$  (the symmetric stretching mode of  $\text{NO}_3^-$ ) shifted to  $1050 \text{ cm}^{-1}$  due to the deliquescence of  $\text{NH}_4\text{NO}_3$ . This measured deliquescence RH (DRH) of  $\text{NH}_4\text{NO}_3$  in this mixed particles is lower than the DRH of  $\text{NH}_4\text{NO}_3$  individually at room temperature, namely  $\sim 62\%$  RH (Ma et al., 2010), indicating that the coexistence of  $\text{H}_2\text{C}_2\text{O}_4$  or calcite can affect the hygroscopic behavior of  $\text{NH}_4\text{NO}_3$ . When the vapor exposure time was increased, peaks due to both  $\text{H}_2\text{C}_2\text{O}_4$  and calcite decreased and finally disappeared. Meanwhile, peaks at 1632, 1491, 1464, 896, 197, and  $140 \text{ cm}^{-1}$  were observed and these peaks were assigned to  $\text{CaC}_2\text{O}_4 \cdot \text{H}_2\text{O}$  according to line d in Fig. 1 (Frost, 2004; Ma and He, 2012). These results suggested that the

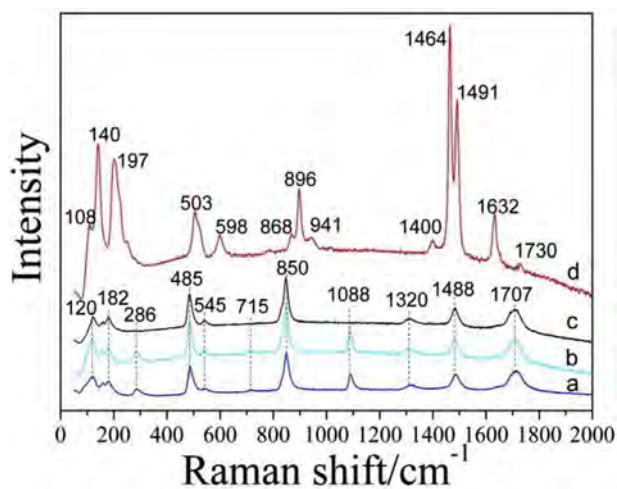


Fig. 1. Comparison of Raman spectra of mixed  $\text{H}_2\text{C}_2\text{O}_4/\text{CaCO}_3$  particles (a) before and (b) after a humidifying-dehumidifying process, (c) anhydrous  $\text{H}_2\text{C}_2\text{O}_4$ , and (d)  $\text{CaC}_2\text{O}_4 \cdot \text{H}_2\text{O}$ .

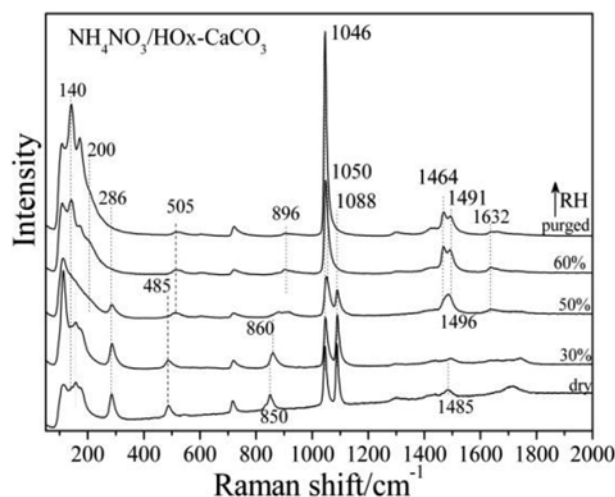


Fig. 2. Raman spectra of mixed 20 wt%  $\text{NH}_4\text{NO}_3\text{-H}_2\text{C}_2\text{O}_4/\text{CaCO}_3$  particles exposed to vapor with different RH and then purged with dry  $\text{N}_2$ .

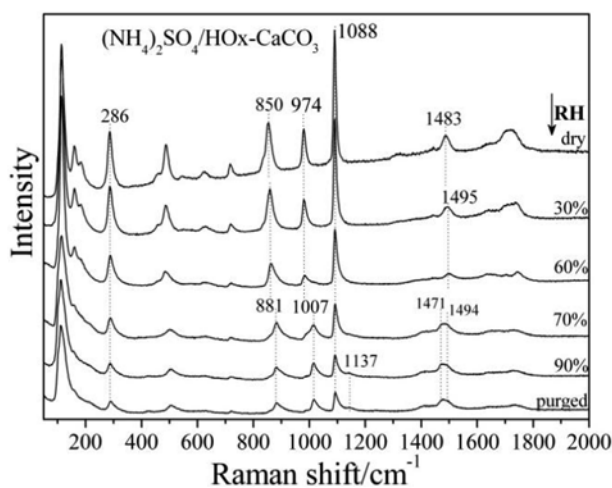


Fig. 3. Raman spectra of mixed 20 wt%  $(\text{NH}_4)_2\text{SO}_4\text{-H}_2\text{C}_2\text{O}_4/\text{CaCO}_3$  particles exposed to vapor with different RH and then purged with dry  $\text{N}_2$ .

consumption of  $\text{H}_2\text{C}_2\text{O}_4$  and calcite took place during the vapor absorption process, resulting in the formation of  $\text{CaC}_2\text{O}_4\cdot\text{H}_2\text{O}$ . When the mixture was purged with dry nitrogen, the intensities of peaks at  $1046\text{ cm}^{-1}$  attributed to  $\text{NH}_4\text{NO}_3$  finally increased. This is due to the deposition of  $\text{NH}_4\text{NO}_3$  on the surface of  $\text{CaC}_2\text{O}_4\cdot\text{H}_2\text{O}$ , since Raman spectroscopy is surface sensitive.

As discussed above, the  $\text{H}^+$  in externally mixed  $\text{H}_2\text{C}_2\text{O}_4$  and  $\text{CaCO}_3$  particles is not available for decomposing calcite in the humidifying process. When hygroscopic components coexist,  $\text{NH}_4\text{NO}_3$  in this case, the deliquescence of  $\text{NH}_4\text{NO}_3$  can dissolve  $\text{H}_2\text{C}_2\text{O}_4$  and release  $\text{H}^+$ , which makes the reaction between  $\text{H}_2\text{C}_2\text{O}_4$  and  $\text{CaCO}_3$  possible. Therefore, in the presence of  $\text{NH}_4\text{NO}_3$ , conversion of  $\text{CaCO}_3$  and  $\text{H}_2\text{C}_2\text{O}_4$  to  $\text{CaC}_2\text{O}_4\cdot\text{H}_2\text{O}$  occurred in the humidifying process.

### 3.3. The effect of $(\text{NH}_4)_2\text{SO}_4$ on the hygroscopic behavior of mixed $\text{CaCO}_3/\text{H}_2\text{C}_2\text{O}_4$ particles

In the case of the 20 wt%  $(\text{NH}_4)_2\text{SO}_4\text{-H}_2\text{C}_2\text{O}_4/\text{CaCO}_3$  mixture, the hygroscopic behavior was different from the case when  $\text{NH}_4\text{NO}_3$  was part of the mixture. As seen in Fig. 3, the peak at  $974\text{ cm}^{-1}$  is attributed to  $(\text{NH}_4)_2\text{SO}_4$  (Ma et al., 2013b). When RH increased to 30%, the conversion of anhydrous  $\text{H}_2\text{C}_2\text{O}_4$  to dihydrate particles was observed as exposure time increased (Ma and He, 2012; Ma et al., 2013a). However, as RH was further increased to 70%, the intensity of the peak at  $1088\text{ cm}^{-1}$  attributed to calcite decreased, indicating consumption of calcite during the humidifying process. Unlike previous results (Ma and He, 2012), peaks belonging to calcium oxalate at 140, 200, and  $900\text{ cm}^{-1}$  were not detected, although two peaks at 1471 and  $1494\text{ cm}^{-1}$  were observed. Meanwhile, several new peaks at 1007 and  $1137\text{ cm}^{-1}$  appeared. These peaks at 1007 and  $1137\text{ cm}^{-1}$  were assigned to the symmetric and asymmetric stretching modes of  $\text{SO}_4^{2-}$  in gypsum (Ma et al., 2013b; Tomic et al., 2010). These results implied that reaction between  $(\text{NH}_4)_2\text{SO}_4$  and  $\text{CaCO}_3$  took place and resulted in the formation of gypsum. On the other hand, the peak at  $860\text{ cm}^{-1}$  attributed to oxalic acid shifted to  $881\text{ cm}^{-1}$ , indicating that  $(\text{NH}_4)_2\text{C}_2\text{O}_4$  formed during the reaction (Frost, 2004). This also implied that  $\text{H}_2\text{C}_2\text{O}_4$  was involved in this reaction.

Although  $\text{H}_2\text{C}_2\text{O}_4$  and  $\text{CaCO}_3$  were prepared with the mole ratio of 1:1,  $\text{CaCO}_3$  in this case was not completely decomposed, unlike in the case with  $\text{NH}_4\text{NO}_3$  present (Fig. 2). There are two possible reasons. Firstly, the reaction between  $(\text{NH}_4)_2\text{SO}_4$  and  $\text{CaCO}_3$  results in the consumption of hygroscopic  $(\text{NH}_4)_2\text{SO}_4$ , and consequently decreases the water content of particles. Thus, the complete dissolution of  $\text{H}_2\text{C}_2\text{O}_4$  as well as decomposition of  $\text{CaCO}_3$  ceased. Secondly, the formation of gypsum on the surface of  $\text{CaCO}_3$  blocks the further reaction of  $\text{CaCO}_3$

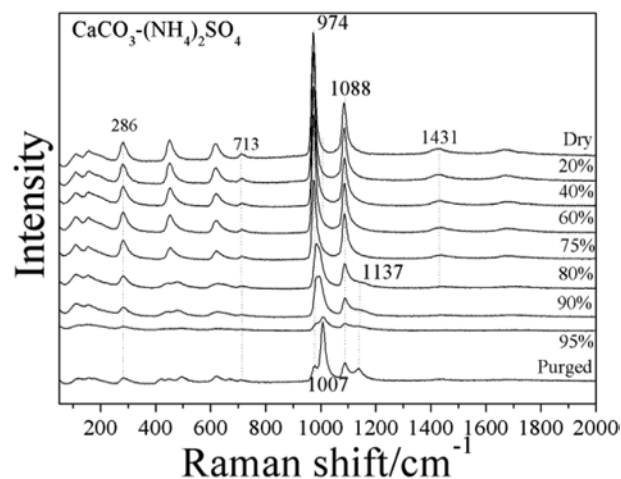


Fig. 4. Raman spectra of mixed  $(\text{NH}_4)_2\text{SO}_4/\text{CaCO}_3$  particles exposed to different RH and then purged with dry  $\text{N}_2$ .

with  $\text{H}_2\text{C}_2\text{O}_4$ , since gypsum is weakly hygroscopic (Gu et al., 2017; Ma et al., 2013b).

To confirm the reaction between  $(\text{NH}_4)_2\text{SO}_4$  and  $\text{CaCO}_3$  during the humidifying process, we further studied the humidifying process of an equi-molar  $(\text{NH}_4)_2\text{SO}_4/\text{CaCO}_3$  mixture. As seen in Fig. 4, the characteristic peaks at  $974$  and  $1088\text{ cm}^{-1}$  were assigned to  $\text{SO}_4^{2-}$  and  $\text{CO}_3^{2-}$ , respectively. When RH increased to 80%, a peak shift from  $974\text{ cm}^{-1}$  to  $981\text{ cm}^{-1}$  was observed due to the deliquescence of  $(\text{NH}_4)_2\text{SO}_4$ . The intensity of the peak at  $1088\text{ cm}^{-1}$  decreased when RH further increased to 95% and then decreased to dry conditions, indicating the decomposition of  $\text{CaCO}_3$  during the deliquescence of co-existing  $(\text{NH}_4)_2\text{SO}_4$ . Meanwhile, two new peaks at  $1007$  and  $1137\text{ cm}^{-1}$  assigned to  $\text{SO}_4^{2-}$  in gypsum were observed. These results confirmed that the chemical reaction between  $\text{CaCO}_3$  and  $(\text{NH}_4)_2\text{SO}_4$  during the humidifying process of mixed particles leads to the formation of gypsum.

### 3.4. The effect of NaCl on the hygroscopic behavior of mixed $\text{CaCO}_3/\text{H}_2\text{C}_2\text{O}_4$ particles

When 20 wt% NaCl was added into mixed  $\text{H}_2\text{C}_2\text{O}_4/\text{calcite}$  particles, a promotion effect on the reaction between  $\text{H}_2\text{C}_2\text{O}_4$  and calcite during the humidifying process could also be observed. Fig. 5 shows the

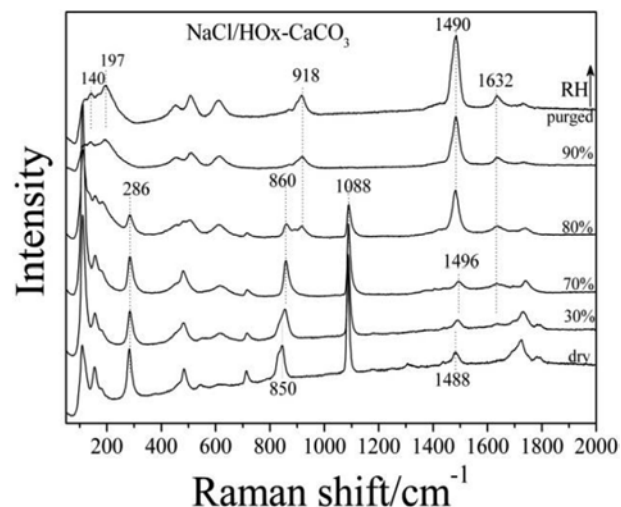


Fig. 5. Raman spectra of mixed 20 wt%  $\text{NaCl-H}_2\text{C}_2\text{O}_4/\text{CaCO}_3$  particles exposed to vapor with different RH and then purged with dry  $\text{N}_2$ .

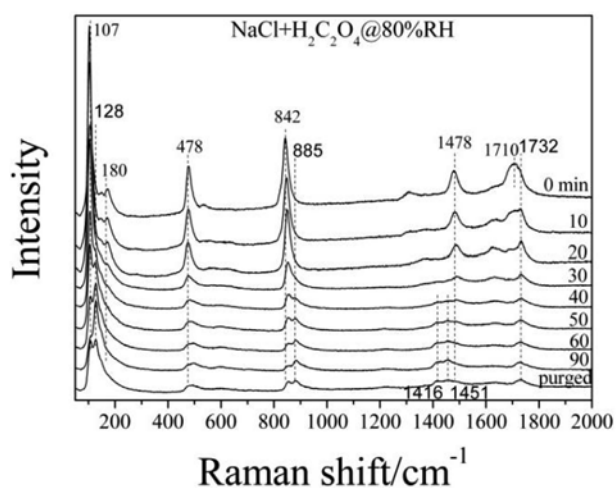


Fig. 6. Raman spectra of mixed NaCl–H<sub>2</sub>C<sub>2</sub>O<sub>4</sub> particles exposed to vapor at 80% RH as a function of time and then purged with dry N<sub>2</sub>.

Raman spectra of mixed 20 wt% NaCl–H<sub>2</sub>C<sub>2</sub>O<sub>4</sub>/CaCO<sub>3</sub> particles exposed to vapor as a function of RH. As RH increased to above 30%, peak positions due to the conversion of anhydrous oxalic acid particles to oxalic acid dihydrate particles was also observed (Ma and He, 2012). As RH further increased to 80%, which is above the deliquescence point of NaCl, *i.e.* 75% RH, the bands attributed to CaCO<sub>3</sub> at 286 and 1088 cm<sup>-1</sup> decreased. These bands finally disappeared after RH increased to 90%. Decrease in the peak intensities of oxalic acid was also detected. Meanwhile, several new peaks at 140, 197, 1490, and 1632 cm<sup>-1</sup> were observed after the dehumidifying process. These peaks can be assigned to CaC<sub>2</sub>O<sub>4</sub>·2H<sub>2</sub>O in the form of weddellite according to Frost and Weier (2003). These results suggest that the presence of coexisting NaCl promoted the reaction between oxalic acid and calcite during the humidifying process.

To investigate whether NaCl was involved in the reaction between CaCO<sub>3</sub> and H<sub>2</sub>C<sub>2</sub>O<sub>4</sub> during the humidifying process, we further studied the humidifying process of a NaCl/H<sub>2</sub>C<sub>2</sub>O<sub>4</sub> mixture with mole ratio of 2:1. As shown in Fig. 6, anhydrous H<sub>2</sub>C<sub>2</sub>O<sub>4</sub> was first converted to dihydrate particles as exposure time increased. Then, a decrease in the peak intensity of H<sub>2</sub>C<sub>2</sub>O<sub>4</sub> was observed, which was due to the solvation effect of the deliquescent NaCl solution. As the exposure time further increased, several new peaks at 128, 885, 1416, 1451, and 1732 cm<sup>-1</sup> were observed. These peaks can be assigned to sodium oxalate particles (Frost, 2004; Ma et al., 2013c). In a previous study, it was demonstrated that replacement of chloride by oxalate occurred in the humidifying process of NaCl and H<sub>2</sub>C<sub>2</sub>O<sub>4</sub> mixtures, because of the weak hygroscopicity of sodium oxalate particles (Ma et al., 2013c). The peak at 918 cm<sup>-1</sup> in Fig. 5 could be assigned neither calcium oxalate nor sodium oxalate, which is possible due to the formation of Na–Ca double oxalate in this system. These results suggested that NaCl was involved in the reaction, rather than simply triggering the reaction by supplying a deliquescent solution. Calcite was completely decomposed in the humidifying process of the NaCl–H<sub>2</sub>C<sub>2</sub>O<sub>4</sub>/CaCO<sub>3</sub> mixture, as seen in Fig. 5, which is different from the case when (NH<sub>4</sub>)<sub>2</sub>SO<sub>4</sub> was present (Fig. 3). This is because the consumption of H<sub>2</sub>C<sub>2</sub>O<sub>4</sub> by reaction with NaCl eventually produced HCl. The HCl formed in the solution can decompose calcite quickly, and residual CaCl<sub>2</sub> may be present in the mixture after dehumidification.

#### 4. Conclusions and atmospheric implications

In this study, the effect of coexisting hygroscopic components on the hygroscopic behavior of mixed H<sub>2</sub>C<sub>2</sub>O<sub>4</sub>/CaCO<sub>3</sub> particles was studied by Raman spectroscopy. It was determined that the existence of hygroscopic components promoted the reaction between H<sub>2</sub>C<sub>2</sub>O<sub>4</sub> and CaCO<sub>3</sub>

during the humidifying process by providing an aqueous environment. These reactions resulted in the formation of insoluble CaC<sub>2</sub>O<sub>4</sub>·H<sub>2</sub>O in the presence of NaCl or NH<sub>4</sub>NO<sub>3</sub>. NH<sub>4</sub>NO<sub>3</sub> exhibited a promotion effect but was not involved in the reaction. In contrast, coexisting (NH<sub>4</sub>)<sub>2</sub>SO<sub>4</sub> had a competition effect on the reaction between H<sub>2</sub>C<sub>2</sub>O<sub>4</sub> and CaCO<sub>3</sub>, and resulted in the formation of CaSO<sub>4</sub>·2H<sub>2</sub>O and (NH<sub>4</sub>)<sub>2</sub>C<sub>2</sub>O<sub>4</sub>. NaCl can react with H<sub>2</sub>C<sub>2</sub>O<sub>4</sub> to form sodium oxalate, which was mixed with calcium oxalate in the final mixed particles.

In general, hygroscopicity is the ability of a substance to attract and hold water molecules from the surrounding environment. It is now well known that the hygroscopic behavior of particles is greatly dependent on their composition. For insoluble particles like calcite, the water adsorption isotherm exhibits a curve typical of multilayer adsorption, and the water content of fresh calcite at 90% RH was determined to be less than 1% (Al-Hosney and Grassian, 2005; Gustafsson et al., 2005; Ma et al., 2012), indicating its hygroscopicity is quite weak. The hygroscopic behavior of calcite particles could be depicted as a water adsorption-desorption process. For oxalic acid, the reported deliquescence point is above 98% RH (Braban et al., 2003), indicating that the deliquescence of oxalic acid rarely happens in the atmosphere since the typical ambient RH is in the range of 20–90%. Unlike calcite, however, the humidifying-dehumidifying process of oxalic acid and other oxalates was determined to be a hydration-dehydration process under typical ambient RH (Braban et al., 2003; Ma and He, 2012; Ma et al., 2013a; Peng et al., 2001; Wu et al., 2011). In the case of hygroscopic compounds, *e.g.* NaCl, NH<sub>4</sub>NO<sub>3</sub>, and (NH<sub>4</sub>)<sub>2</sub>SO<sub>4</sub>, water absorption at DRH makes these particles mainly occur in a metastable state in the atmosphere (Ma et al., 2010; Martin, 2000; Rood et al., 1989; Schuttlefield et al., 2007; Swietlicki et al., 2008). This results in the dissolution of particles, with cations and anions that re-combine together after efflorescence. Thus, the hygroscopic behavior of hygroscopic particles is always a dissolution-recrystallization process, namely deliquescence and efflorescence. The traditional view always considers the hygroscopic behavior of aerosol mixtures particles as a physically vapor adsorption/absorption-desorption process, in which chemical reaction is neglected. However, as shown in this study, chemical reactions may occur in the humidifying process of mixed particles. In the case of CaCO<sub>3</sub>, coexisting hygroscopic components can greatly increase its water content after the deliquescence of these hygroscopic components. The aqueous circumstance can promote the chemical reaction between CaCO<sub>3</sub> and acidic species (*e.g.*, H<sub>2</sub>C<sub>2</sub>O<sub>4</sub>) in the atmosphere. Moreover, the formation of insoluble or less hygroscopic components in the aqueous chemical reaction in the humidification-dehumidification process will change the hygroscopic behavior as well as climate effect of particles.

#### Declaration of interest statement

The authors have no competing interests to declare.

#### Acknowledgements

Laboratory of This research was financially supported by the National Key R&D Program of China, China (2016YFC0202700) and the National Natural Science Foundation of China, China (21876185, 91744205). The authors also appreciate the Youth Innovation Promotion Association, CAS, China (2018055) and the special fund of the State Key Joint Laboratory of Environment Simulation and Pollution Control, China (17L01ESPC).

#### Appendix A. Supplementary data

Supplementary data to this article can be found online at <https://doi.org/10.1016/j.atmosenv.2018.11.056>.

## References

- Al-Abadleh, H.A., Krueger, B.J., Ross, J.L., Grassian, V.H., 2003. Phase transitions in calcium nitrate thin films. *Chem. Commun.* 22, 2796–2797.
- Al-Hosney, H.A., Grassian, V.H., 2005. Water, sulfur dioxide and nitric acid adsorption on calcium carbonate: a transmission and ATR-FTIR study. *Phys. Chem. Chem. Phys.* 7, 1266–1276.
- Andreae, M.O., Charlson, R.J., Bruynseels, F., Storms, H., Van Grieken, R., Maenhaut, W., 1986. Internal mixture of sea salt, silicates, and excess sulfate in marine aerosols. *Science* 232, 1620–1623.
- Braban, C.F., Abbatt, J.P.D., 2004. A study of the phase transition behavior of internally mixed ammonium sulfate-malonic acid aerosols. *Atmos. Chem. Phys.* 4, 1451–1459.
- Braban, C.F., Carroll, M.F., Styler, S.A., Abbatt, J.P.D., 2003. Phase transitions of malonic and oxalic acid aerosols. *J. Phys. Chem.* 107, 6594–6602.
- Brooks, S., Wise, M., Cushing, M., Tolbert, M., 2002. Deliquescence behavior of organic/ammonium sulfate aerosol. *Geophys. Res. Lett.* 29, 1917.
- Chan, C.K., Ha, Z., Choi, M.Y., 2000. Study of water activities of aerosols of mixtures of sodium and magnesium salts. *Atmos. Environ.* 34, 4795–4803.
- Charlson, R.J., Schwartz, S.E., Hales, J.M., Cess, R.D., Coakley, J.A., Hansen, J.E., Hofmann, D.J., 1992. Climate forcing by anthropogenic aerosols. *Science* 255, 423–430.
- Chebbi, A., Carlier, P., 1996. Carboxylic acids in the troposphere, occurrence, sources, and sinks: a review. *Atmos. Environ.* 30, 4233–4249.
- Choi, M.Y., Chan, C.K., 2002. The effects of organic species on the hygroscopic behaviors of inorganic aerosols. *Environ. Sci. Technol.* 36, 2422–2428.
- Crowley, J.N., Ammann, M., Cox, R.A., Hynes, R.G., Jenkin, M.E., Mellouki, A., Rossi, M.J., Troe, J., Wallington, T.J., 2010. Evaluated kinetic and photochemical data for atmospheric chemistry: volume V—heterogeneous reactions on solid substrates. *Atmos. Chem. Phys.* 10, 9059–9223.
- Cruz, C.N., Pandis, S.N., 2000. Deliquescence and hygroscopic growth of mixed inorganic-organic atmospheric aerosol. *Environ. Sci. Technol.* 34, 4313–4319.
- Dentener, F.J., Carmichael, G.R., Zhang, Y., Lelieveld, J., Crutzen, P.J., 1996. Role of mineral aerosol as a reactive surface in the global troposphere. *J. Geophys. Res.* 101 (22) 869–822,889.
- Drozd, G., Woo, J., Häkkinen, S.A.K., Nenes, A., McNeill, V.F., 2014. Inorganic salts interact with oxalic acid in submicron particles to form material with low hygroscopicity and volatility. *Atmos. Chem. Phys.* 14, 5205–5215.
- Frost, R.L., 2004. Raman spectroscopy of natural oxalates. *Anal. Chim. Acta* 517, 207–214.
- Frost, R.L., Weier, M.L., 2003. Raman spectroscopy of natural oxalates at 298 and 77 K. *J. Raman Spectrosc.* 34, 776–785.
- Furukawa, T., Takahashi, Y., 2011. Oxalate metal complexes in aerosol particles implications for the hygroscopicity of oxalate-containing particles. *Atmos. Chem. Phys.* 11, 4289–4301.
- Gierlus, K.M., Laskina, O., Abernathy, T.L., Grassian, V.H., 2012. Laboratory study of the effect of oxalic acid on the cloud condensation nuclei activity of mineral dust aerosol. *Atmos. Environ.* 46, 125–130.
- Gu, W.J., L, Y.J., Zhu, J.X., Jia, X.H., Lin, Q.H., Zhang, G.H., Ding, X., Song, W., Bi, X.H., Wang, X.M., et al., 2017. Investigation of water adsorption and hygroscopicity of atmospherically relevant particles using a commercial vapor sorption analyzer. *Atmos. Meas. Tech.* 10, 3821–3832.
- Gustafsson, R.J., Orlov, A., Badger, C.L., Griffiths, P.T., Cox, R.A., Lambert, R.M., 2005. A comprehensive evaluation of water uptake on atmospherically relevant mineral surfaces: DRIFT spectroscopy, thermogravimetric analysis and aerosol growth measurements. *Atmos. Chem. Phys.* 5, 3415–3421.
- Hallquist, M., Wenger, J., Baltensperger, U., Rudich, Y., Simpson, D., Claeys, M., Dommen, J., Donahue, N., George, C., Goldstein, A., 2009. The formation, properties and impact of secondary organic aerosol: current and emerging issues. *Atmos. Chem. Phys.* 9, 5155–5236.
- Laskin, A., Iedema, M.J., Ichkovich, A., Graber, E.R., Taraniuk, I., Rudich, Y., 2005. Direct observation of completely processed calcium carbonate dust particles. *Faraday Discuss* 130, 453–468.
- Laskin, A., Moffet, R.C., Gilles, M.K., Fast, J.D., Zaveri, R.A., Wang, B.B., Nigge, P., Shuthanandan, J., 2012. Tropospheric chemistry of internally mixed sea salt and organic particles: surprising reactivity of NaCl with weak organic acids. *J. Geophys. Res.* D15302.
- Laskina, O., Morris, H.S., Grandquist, J.R., Qin, Z., Stone, E.A., Tivanski, A.V., Grassian, V.H., 2015. Size matters in the water uptake and hygroscopic growth of atmospherically relevant multicomponent aerosol particles. *J. Phys. Chem.* 119, 4489–4497.
- Laskina, O., Young, M.A., Kleiber, P.D., Grassian, V.H., 2013. Infrared extinction spectroscopy and micro-Raman spectroscopy of select components of mineral dust mixed with organic compounds. *J. Geophys. Res.* 119, 1–14.
- Li, W.J., Shao, L.Y., 2009a. Observation of nitrate coatings on atmospheric mineral dust particles. *Atmos. Chem. Phys.* 9, 1863–1871.
- Li, W.J., Shao, L.Y., 2009b. Transmission electron microscopy study of aerosol particles from the brown hazes in northern China. *J. Geophys. Res.* 114, D09302.
- Liu, Y., Liu, C., Ma, J., Ma, Q., He, H., 2010. Structural and hygroscopic changes of soot during heterogeneous reaction with O<sub>3</sub>. *Phys. Chem. Chem. Phys.* 12 (10) 896–810,903.
- Liu, Y.J., Zhu, T., Zhao, D.F., Zhang, Z.F., 2008. Investigation of the hygroscopic properties of Ca(NO<sub>3</sub>)<sub>2</sub> and internally mixed Ca(NO<sub>3</sub>)<sub>2</sub>/CaCO<sub>3</sub> particles by micro-Raman spectrometry. *Atmos. Chem. Phys.* 8, 7205–7215.
- Ma, Q., He, H., 2012. Synergistic effect in the humidifying process of atmospheric relevant calcium nitrate, calcite and oxalic acid mixtures. *Atmos. Environ.* 50, 97–102.
- Ma, Q., He, H., Liu, C., 2013a. Hygroscopic properties of oxalic acid and atmospherically relevant oxalates. *Atmos. Environ.* 69, 281–288.
- Ma, Q., He, H., Liu, Y., Liu, C., Grassian, V.H., 2013b. Heterogeneous and multiphase formation pathways of gypsum in the atmosphere. *Phys. Chem. Chem. Phys.* 15, 19196–19204.
- Ma, Q., Liu, Y., He, H., 2010. The utilization of physisorption analyzer for studying the hygroscopic properties of atmospheric relevant particles. *J. Phys. Chem.* 114, 4232–4237.
- Ma, Q., Liu, Y., Liu, C., He, H., 2012. Heterogeneous reaction of acetic acid on MgO, α-Al<sub>2</sub>O<sub>3</sub>, and CaCO<sub>3</sub> and the effect on the hygroscopic behaviour of these particles. *Phys. Chem. Chem. Phys.* 14, 8403–8409.
- Ma, Q., Ma, J., Liu, C., Lai, C., He, H., 2013c. Laboratory study on the hygroscopic behavior of external and internal C2-C4 dicarboxylic acid-NaCl mixtures. *Environ. Sci. Technol.* 47, 10381–10388.
- Martin, S.T., 2000. Phase transitions of aqueous atmospheric particles. *Chem. Rev.* 100, 3403–3453.
- Peng, C., Chan, M.N., Chan, C.K., 2001. The hygroscopic properties of dicarboxylic and multifunctional acids: measurements and UNIFAC predictions. *Environ. Sci. Technol.* 35, 4495–4501.
- Pilinis, C., Pandis, S.N., Seinfeld, J.H., 1995. Sensitivity of direct climate forcing by atmospheric aerosols to aerosol size and composition. *J. Geophys. Res.* 100 (18) 739–718,754.
- Pope, F.D., Dennis-Smith, B.J., Griffiths, P.T., Clegg, S.L., Cox, R.A., 2010. Studies of single aerosol particles containing malonic acid, glutaric acid, and their mixtures with sodium chloride. I. Hygroscopic growth. *J. Phys. Chem.* 114, 5335–5341.
- Poschl, U., 2005. Atmospheric aerosols: composition, transformation, climate and health effects. *Angew. Chem. Int. Ed.* 44, 7520–7541.
- Prenni, A.J., DeMott, P.J., Kreidenweis, S.M., 2003. Water uptake of internally mixed particles containing ammonium sulfate and dicarboxylic acids. *Atmos. Environ.* 37, 4243–4251.
- Ramanathan, V., Crutzen, P.J., Kiehl, J.T., Rosenfeld, D., 2001. Aerosols, climate, and the hydrological cycle. *Science* 294, 2119–2124.
- Rood, M., Shaw, M., Larson, T., Covert, D., 1989. Ubiquitous nature of ambient metastable aerosol. *Nature* 537–539.
- Schuttlefield, J., Al-Hosney, H., Zachariah, A., Grassian, V.H., 2007. Attenuated total reflection Fourier transform infrared spectroscopy to investigate water uptake and phase transitions in atmospherically relevant particles. *Appl. Spectrosc.* 61, 283–292.
- Shao, X., Wu, F.-M., Yang, H., Pang, S.-F., Zhang, Y.-H., 2018. Observing HNO<sub>3</sub> release dependent upon metal complexes in malonic acid/nitrate droplets. *Spectrochim. Acta Mol. Biomol. Spectrosc.* 201, 399–404.
- Solomon, S., Qin, Dahe, Manning, Martin, Chen, Zhenlin, Marquis, Melinda, Averyt, K.B., Tignor, Melinda, Miller, H.L., 2007. Climate Change 2007: the Physical Science Basis. Contribution of Working Group I to the Fourth Assessment Report of the Intergovernmental Panel on Climate Change.
- Sullivan, R.C., Guazzotti, S.A., Sodeman, D.A., Prather, K.A., 2007. Direct observations of the atmospheric processing of Asian mineral dust. *Atmos. Chem. Phys.* 7, 1213–1236.
- Sullivan, R.C., Prather, K.A., 2007. Investigations of the diurnal cycle and mixing state of oxalic acid in individual particles in Asian aerosol outflow. *Environ. Sci. Technol.* 41, 8062–8069.
- Swietlicki, E., Hansson, H., Hameri, K., Svenningsson, B., Massling, A., McFiggans, G., McMurry, P., Petaja, T., Tunved, P., Gysel, M., 2008. Hygroscopic properties of submicrometer atmospheric aerosol particles measured with H-TDMA instruments in various environments: a review. *Tellus B* 60, 432–469.
- Tang, I.N., Fung, K.H., 1997. Hydration and Raman-scattering studies of levitated microparticles: Ba(NO<sub>3</sub>)<sub>2</sub>, Sr(NO<sub>3</sub>)<sub>2</sub>, and Ca(NO<sub>3</sub>)<sub>2</sub>. *J. Chem. Phys.* 106, 1653–1660.
- Tang, M.J., Chen, J., Wu, Z.J., 2018. Ice nucleating particles in the troposphere: progresses, challenges and opportunities. *Atmos. Environ.* 192, 206–208.
- Tang, M.J., Cziczo, D.J., Grassian, V.H., 2016. Interactions of water with mineral dust aerosol: water adsorption, hygroscopicity, cloud condensation and ice nucleation. *Chem. Rev.* 116, 4205–4259.
- Tomic, Z., Makreski, P., Gajic, B., 2010. Identification and spectra-structure determination of soil minerals: Raman study supported by IR spectroscopy and X-ray powder diffraction. *J. Raman Spectrosc.* 41, 582–586.
- Usher, C.R., Michel, A.E., Grassian, V.H., 2003. Reactions on mineral dust. *Chem. Rev.* 103, 4883–4940.
- Wang, B., Laskin, A., 2014. Reactions between water-soluble organic acids and nitrates in atmospheric aerosols: recycling of nitric acid and formation of organic salts. *J. Geophys. Res.* Atmos. 119, 3335–3351.
- Wang, G., Kawamura, K., Cheng, C., Li, J., Cao, J., Zhang, R., Zhang, T., Liu, S., Zhao, Z., 2012. Molecular distribution and stable carbon isotopic composition of dicarboxylic acids, ketocarboxylic acids, and α-dicarbonyls in size-resolved atmospheric particles from Xi'an city, China. *Environ. Sci. Technol.* 46, 4783–4791.
- Wang, X., Jing, B., Tan, F., Ma, J., Zhang, Y., Ge, M., 2017. Hygroscopic behavior and chemical composition evolution of internally mixed aerosols composed of oxalic acid and ammonium sulfate. *Atmos. Chem. Phys.* 17, 12797–12812.
- Wise, M.E., Surratt, J.D., Curtis, D.B., Shilling, J.E., Tolbert, M.A., 2003. Hygroscopic growth of ammonium sulfate/dicarboxylic acids. *J. Geophys. Res.* 108, 4638.
- Wu, Z.J., Nowak, A., Poulain, L., Herrmann, H., Wiedensohler, A., 2011. Hygroscopic behavior of atmospherically relevant water-soluble carboxylic salts and their influence on the water uptake of ammonium sulfate. *Atmos. Chem. Phys.* 11, 12617–12626.
- Yang, F., Chen, H., Wang, X.N., Yang, X., Du, J.F., Chen, J.M., 2009. Single particle mass spectrometry of oxalic acid in ambient aerosols in Shanghai: mixing state and formation mechanism. *Atmos. Environ.* 43, 3876–3882.